UNCLASSIFIED

AD NUMBER	
AD311158	
CLASSIFICATION CHANGES	
TO:	**unclassified**
FROM:	**confidential**
LIMITATION CHANGES	
TO: **Approved for public release; distribution is unlimited.**	
FROM: **Distribution authorized to DoD only; Administrative/Operational Use; SEP 1963. Other requests shall be referred to Defense Atomic Support Agency, Albuquerque, NM.**	
AUTHORITY	
DNA/SSTL ltr dtd 14 Sep 1995; DNA/SSTL ltr dtd 14 Sep 1995	

THIS PAGE IS UNCLASSIFIED

Postal Registry No. 15669

CONFIDENTIAL

ITR-1437

This document consists of 33 pages.

No. 187 of 265 copies, Series A

PRELIMINARY REPORT

OPERATION
PLUMBBOB

NEVADA TEST SITE
MAY-SEPTEMBER 1957

Project 6.3

ATTENUATION OF ELECTROMAGNETIC RADIATION THROUGH AN IONIZED MEDIUM

HEADQUARTERS FIELD COMMAND,
ARMED FORCES SPECIAL WEAPONS PROJECT
SANDIA BASE, ALBUQUERQUE, NEW MEXICO

FORMERLY RESTRICTED DATA

Handle as Restricted Data in foreign dissemination. Section 144b, Atomic Energy Act of 1954.

This material contains information affecting the national defense of the United States within the meaning of the espionage laws Title 18, U. S. C., Secs. 793 and 794, the transmission or revelation of which in any manner to an unauthorized person is prohibited by law.

CONFIDENTIAL

This is a preliminary report based on all data available at the close of this project's participation in Operation PLUMBBOB. The contents of this report are subject to change upon completion of evaluation for the final report. This preliminary report will be superseded by the publication of the final (WT) report. Conclusions are recommendations drawn herein, if any, are therefore tentative. The work is reported at this early time to provide early test results to those concerned with the effects of nuclear weapons and to provide for an interchange of information between projects for the preparation of final reports.

AEC Technical Information Service Extension
Oak Ridge, Tennessee

AD-311158

ITR–1437

OPERATION PLUMBBOB–PROJECT 6.3

ATTENUATION OF ELECTROMAGNETIC RADIATION THROUGH AN IONIZED MEDIUM

William S. Lee

U. S. Naval Air Development Center
Johnsville, Pennsylvania

Issuance Date: September 13, 1957

FORMERLY RESTRICTED DATA

Handle as Restricted Data in foreign dissemination. Section 144b, Atomic Energy Act of 1954.

This material contains information affecting the national defense of the United States within the meaning of the espionage laws Title 18, U. S. C., Secs. 793 and 794, the transmission or revelation of which in any manner to an unauthorized person is prohibited by law.

H. Black
H. Black, Lt Col, USA
Director, Program 6

K.D. Coleman
K. D. Coleman, Col, USAF
Test Group Director, Programs 1–9

ABSTRACT

The objectives of Project 6.3 were to measure the attenuation of electromagnetic radiation of various frequencies due to propagation through an ionized cloud, and to compute the rate of removal of electrons by recombination and attachment from the attenuation measurements.

Radio signals propagated through an ionized cloud for yields up to 9.6 kt, from one to four minutes after the detonation, were not attenuated.

An M-33 X-band fire-control radar skin tracked an FJ aircraft through the ionized cloud from a 40-kt detonation. No difference in signal level was noted whether or not the ionized cloud was interposed between the radar and the aircraft.

FOREWORD

This report presents the preliminary results of one of the 43 projects comprising the Military Effects Program of Operation Plumbbob, which included 28 test detonations at the Nevada Test Site in 1957.

For overall Plumbbob military-effects information, the reader is referred to the "Summary Report of the Director, DOD Test Group (Programs 1–9)," ITR–1445, which includes: (1) a description of each detonation, including yield, zero-point location and environment, type of device, ambient atmospheric conditions, etc.; (2) a discussion of project results; (3) a summary of the objectives and results of each project; and (4) a listing of project reports for the Military Effects Program.

PREFACE

Dr. Ralph Zirkind of the Bureau of Aeronautics, Navy Department, Washington, D. C. is responsible for the theory in Section 1.3 of this report.

The U. S. Naval Air Special Weapons Facility Detachment supplied the aircraft, pilots, M–33 radar, and the aircraft controller in support of this project.

CONTENTS

FIGURES

TABLES

Chapter 1

INTRODUCTION

1.1 OBJECTIVES

The objectives of Project 6.3 were: (1) to measure the attenuation of electromagnetic radiation of various frequencies due to propagation through an ionized cloud from a nuclear detonation, and (2) to compute the rate of removal of electrons by recombination and attachment from the attenuation measurements.

1.2 BACKGROUND

The attenuation of electromagnetic radiation through ionized media has been reported previously (Reference 1). Radioactivity produces an electron atmosphere different from free space, thereby attenuating incident radiation. Results from Operation Redwing (Reference 1) indicate that at low frequencies (4 to 8 Mc) complete blackout or strong perturbation of the transmitted signal occurred for yields in excess of 250 kt. For lower yields and other frequencies little data exists. In Reference 2, it is reported that X-band (9,375-Mc) energy suffered strong attenuation at times of the order of microseconds after the blast. For Redwing Shot Inca, the attenuation persisted in a sporadic fashion for at least 10 seconds (end of recording time) after the detonation (Reference 2). Measurements for kiloton-range detonations at later periods of time after the detonation have not been made. Serious operational implications are evident if attenuation occurs; e.g. loss of radio contact.

1.3 THEORY

The attenuation of an electromagnetic signal transmitted through a radioactive cloud from a nuclear detonation can be considered to be a result of the excess electrons from the fission-product gamma and beta radiation.

Consider a medium having N_ϵ free electrons per cubic centimeter with velocity $\bar{V}$ acted upon by an external force:

$$e\,\bar{\bar{E}}_o{}^{-i\omega t}$$

Then, in the absence of a magnetic field,[1] the equation of motion is (Reference 3):

$$\frac{m d\bar{V}}{dt} + \frac{m\bar{V}}{\tau} = e\,\bar{\bar{E}}_o{}^{-i\omega t} \qquad (1.1)$$

---

[1] Emission of electrons is isotropic; therefore the magnetic field merely rearranges directions but not average number per unit volume.

Where: $\frac{-m\bar{V}}{t}$ = opposing force[2]

m = electron mass

τ = mean free time between collisions

$\bar{E}_o$ = amplitude of electric field

ω = angular frequency of electric field

e = electron charge

The steady state solution of equation 1.1 is:

$$\bar{V} = \frac{e\,\bar{E}_o^{\,-i\omega t}}{m\left(\frac{1}{\tau} - i\omega\right)} \tag{1.2}$$

The current density $\bar{j}$ for N_ϵ free electrons per cubic centimeter moving with velocity $\bar{V}$ is:

$$\bar{j} = N_\epsilon e \bar{V} = \frac{N_\epsilon e^2 \bar{E}}{m\,(\frac{1}{\tau} - i\omega)} = \frac{N_\epsilon e^2 \bar{E}\left(\frac{1}{\tau} + i\omega\right)}{m\left(\frac{1}{\tau^2} + \omega^2\right)} \tag{1.3}$$

Where: $\bar{E}$ = root-mean-square value of the electric field.

The complex conductivity σ' is defined by:

$$\sigma' = \frac{\bar{j}}{\bar{E}} = \frac{N_\epsilon e^2 \tau (1 + i\omega\tau)}{m\,(1 + \tau^2 \omega^2)} \tag{1.4}$$

From electromagnetic theory, the complex propagation factor k is defined by the relation:

$$k^2 = (\alpha + i\beta)^2 = \frac{\omega^2}{c^2}\left(1 + \frac{i\sigma'}{\omega\epsilon_o}\right) \tag{1.5}$$

Where: α = phase constant

β = attenuation coefficient

ϵ_o = permittivity of free space ($\frac{1}{4\pi}$ in Gaussian units)

c = speed of light

If Equation 1.4 is substituted into Equation 1.5 and real and imaginary parts are equated, the following results are obtained:

---

[2] The term $\frac{m}{\tau}$ has the dimensions of $\frac{\text{mass}}{\text{time}}$. It has been justified to be sufficiently accurate for experimental purposes (Reference 4).

$$\alpha^2 - \beta^2 = \frac{\omega^2}{c^2}\left[1 - \frac{N_\epsilon \tau^2 e^2}{\epsilon_o m\,(1 + \omega^2 \tau^2)}\right] \tag{1.6a}$$

$$2\,\alpha\beta = \frac{\omega^2}{c^2}\left[\frac{N_\epsilon \tau e^2}{\omega \epsilon_o m\,(1 + \omega^2 \tau^2)}\right] \tag{1.6b}$$

Equations 1.6a and 1.6b can be solved simultaneously for β^2 with the following result:

$$\beta^2 = \frac{\omega^2}{2c^2}\left\{ - \left(1 - \frac{N_\epsilon e^2 \tau^2}{\epsilon_o m (1 + \omega^2 \tau^2)}\right) + \left[\left(1 - \frac{N_\epsilon e^2 \tau^2}{\epsilon_o m (1 + \omega^2 \tau^2)}\right)^2 + \left(\frac{N_\epsilon e^2 \tau}{\omega \epsilon_o m (1 + \omega^2 \tau^2)}\right)^2\right]^{1/2}\right\} \tag{1.7}$$

The positive value of β^2 is taken to ensure a real value for the attenuation coefficient. To convert from power loss in nepers (the units of β) to power loss in decibels, the following relation applies:

$$\text{Power Loss} = 8.686\,\beta \text{ db/cm} \tag{1.8}$$

The terms τ and N_ϵ in Equation 1.4 will now be defined. From kinetic theory (Reference 5) the mean free path λ_m for a molecule is given by

$$\lambda_m = \frac{1}{\sqrt{2}\,\pi n d^2} \tag{1.9}$$

Where: n = number of molecules/cm^3
d = mean molecular diameter (3×10^{-8} cm)

The mean free path λ_e for a free electron is related to the molecular mean free path by:

$$\lambda_e = 4\sqrt{2}\,\lambda m \tag{1.10}$$

If Equation 1.10 is substituted into Equation 1.9 the following is obtained

$$\lambda_e = \frac{4}{\pi n d^2} \tag{1.10a}$$

For a gas having a Boltzman distribution (Reference 5) the average velocity is given by:

$$V_{av} = \frac{8KT}{\pi m} \tag{1.11}$$

Where: K = Boltzman's constant (1.38×10^{-16} erg/deg)
T = Absolute temperature in degrees Kelvin

The collision frequency is by definition:

$$\nu = \frac{V_{av}}{\lambda_e} \tag{1.12}$$

Upon substitution of Equations 1.10a and 1.11, Equation 1.12 becomes:

$$\nu = nd^2 \left(\frac{\pi KT}{2m}\right)^{1/2} \tag{1.13}$$

If it is assumed that T is 300° K:

$$\nu = \frac{1}{\tau} = 7.6 \times 10^{-9} n \tag{1.14}$$

Where: $\frac{n}{\sigma} = 2.6 \times 10^{19}/\text{cm}^3$ (Reference 5)

$$\sigma = \frac{\text{Ambient Density at Altitude}}{\text{Ambient Density at Sea Level}}$$

By Reference 6:

$$\sigma = (1 - 6.88 \times 10^{-6} h)^{4.256} \tag{1.15}$$

Where: h = altitude in feet above sea level

The radioactive cloud associated with an atomic detonation consists primarily of fission products mixed with surface contaminants. In determining the electron density, the simplifying assumption that the cloud is a uniform mixture of fission products will be made. These fission products emit gamma rays and beta particles, which in turn ionize the surrounding air and thereby produce electrons.

The number of beta particles emitted per second per kiloton, t minutes after fission (Reference 7), is given by:

$$N_\beta = \frac{9.12 \times 10^{20} Y}{t^{1.2}} \tag{1.16}$$

Where: Y = total yield in kilotons

The mean energy of the fission-product betas is approximately 0.4 Mev (Reference 8). Since it requires about 32.5 ev per ion pair at sea-level pressures (Reference 7) and the range of the beta particles is about 1.5 meters (Reference 8), about 82 electrons per centimeter of path will be formed for each beta particle emitted.

The number of gamma rays emitted per second per kiloton, t minutes after fission, is given by (Reference 8):

$$N_\gamma = \frac{4.56 \times 10^{20} \gamma}{t^{1.2}} \tag{1.17}$$

The mean energy of the gamma rays is approximately 0.7 Mev (Reference 8). It is shown in Reference 7 that each gamma will produce approximately 0.8 electrons.

The cloud volume will now be defined as a function of time. In Reference 8 the ionized cloud dimensions are given as:

$$\text{Horizontal Diameter} = 6.8 \times 10^4 Y^{0.2} t^{0.3} \text{ (cm)} \tag{1.18a}$$

$$\text{Vertical Thickness} = 2.27 \times 10^{4} Y^{0.2} t^{0.2} \text{ (cm)} \tag{1.18b}$$

Where: Y = yield of device in kilotons
t = time in minutes after detonation

If the cloud is considered to be an oblate spheroid, its volume is:

$$V = \frac{4}{3}\pi \left(3.4 \times 10^{4} Y^{0.2} t^{0.3}\right)^{2} \left(1.14 \times 10^{4} Y^{0.2} t^{0.2}\right)$$

$$= 5.5 \times 10^{13} Y^{0.6} t^{0.8} \tag{1.19}$$

By combining Equations 1.16, 1.17, and 1.19 with the number of electrons produced per centimeter of path, the production rate P of electrons per cubic centimeter, t minutes after detonation, at sea-level density is:

$$P = \frac{9.12 \times 10^{20} Y}{t^{1.2}} \times \frac{82 \times 1.5 \times 10^{2}}{5.5 \times 10^{13} Y^{0.6} t^{0.8}} + \frac{4.56 \times 10^{20} Y}{t^{1.2}} \times \frac{0.8}{5.5 \times 10^{13} Y^{0.6} t^{0.8}} \approx \frac{2 \times 10^{11} Y^{0.4}}{t^{2}} \tag{1.20}$$

The contribution from gamma rays is insignificant in comparison with that from beta particles.

Electron production and attachment are dependent upon the gas density within the cloud. It will be assumed that the density within the cloud is equivalent to the ambient atmospheric density. From Reference 9, the height of the cloud H above the point of detonation as a function of time is:

$$H = 4600 \, Y^{0.2} \, t^{0.9} \text{ (ft)} \tag{1.21}$$

The exponent of t in Equation 1.21 is valid for $t \leq 30$ seconds after detonation. For later times the cloud rises at a slower rate and a more appropriate relation is,[3] for $t > 30$ seconds:

$$H = 4600 \, Y^{0.2} \, t^{0.53} \text{ (ft)} \tag{1.22}$$

Upon substituting Equation 1.22 into Equation 1.15, the following is obtained:

$$\sigma = \left[1 - (6.88 \times 10^{-6}) \left(Z + 4600 \, Y^{0.2} \, t^{0.53}\right)\right]^{4.256} \tag{1.23}$$

Where: Z = height of burst in feet above sea level

---

[3] This is an interpolation by R. Zirkind between Equation 1.21 and data from Reference 10.

The equation for the instantaneous electron density $N_\epsilon(t)$ can now be written. From a conservation equation, the time derivative of the electron density is:

$$\frac{d\,N_\epsilon\,(t)}{dt} = \text{Production Rate} - \text{Removal Rate} \tag{1.24}$$

As previously stated, the production rate indicated in Equation 1.20 is proportional to the gas density. Since the recombination process can be neglected (Reference 11), the only removal process considered here is electron attachment, which is also proportional to the gas density.

Hence, substitution of Equation 1.20 into Equation 1.24 yields:

$$\frac{d\,N_\epsilon\,(t)}{dt} = \frac{\sigma \times 2 \times 10^{13}\,Y^{0.4}}{t^2} - \sigma\,a\,N_\epsilon\,(t) \tag{1.25}$$

Where: σ is defined by Equation 1.23

a = attachment rate at sea level
t = time in minutes after detonation

The above analysis is valid until the cloud reaches its stabilized altitude. (30 seconds $< t \leq 7$ minutes). For $t > 7$ minutes, the volume of the cloud must be determined experimentally for the particular cloud investigated and the production rate in Equation 1.20 modified accordingly. Furthermore, after the cloud reaches its stabilized altitude, σ will be a numerical constant. Lastly, it is assumed that fallout of fission products does not occur; within the observation period of Project 6.3, this assumption will introduce little error.

Chapter 2

PROCEDURE

2.1 OPERATIONS

It was planned that Project 6.3 would participate only in shots of less than 10-kt yield, because for the larger-yield devices the A4D-1 and FJ aircraft used were committed to aircraft effects projects. Specifically, the project participated in Shots Franklin, Lassen, and Wilson using the A4D-1 aircraft, and in Shots Franklin and Priscilla using the FJ aircraft.

The first and primary part of the operational phase was designed to measure the attenuation of electromagnetic energy propagated through the ionized nuclear cloud. The second part was designed to check the ability of an M-33 X-band radar to skin track an aircraft while the aircraft was screened from the radar by an ionized cloud.

2.1.1 Attenuation Measurement. To obtain attenuation measurements, the A4D-1 aircraft carrying transmitters tuned to six different frequencies from 4 Mc to 9,245 Mc was positioned at H + 1 minute, so that the ionized cloud was on a straight line between the aircraft and a set of ground-based receivers. Between H + 1 and H + 4 minutes, the aircraft was flown toward the ground receivers along a course that kept the cloud directly between the aircraft and the receivers. Radio signals transmitted from the aircraft through the cloud to the receivers were recorded at the receiver site and compared to recordings taken on a calibration run made immediately prior to the shot.

The initial position of the aircraft was determined, based upon the predicted locations of the cloud at H + 1 minute. From H + 1 to H + 4 minutes the pilot positioned the aircraft by observing flares of 3×10^6 candlepower set off at the receiver site. On the Franklin and Lassen shots, the cloud density was thin enough for the pilot to observe the flares directly through the cloud. On the Wilson shot, the pilot maintained the proper aircraft position by keeping the flares screened from his vision by the cloud.

To make the preshot calibration run and in case weather conditions prevented the pilot from visually positioning the aircraft, flight patterns were computed to be used by the M-33 radar controller to position the aircraft. These patterns were computed as late as possible prior to zero time to take into account the latest predicted locations of the ionized cloud for the time interval from H + 1 to H + 4 minutes. Figures 2.1, 2.2, and 2.3 show the flight patterns for the A4D-1 aircraft for Shots Franklin, Lassen, and Wilson prior to their correction to account for the drift of the cloud due to wind.

2.1.2 Radar Skin Tracking. To accomplish the second part of the experiment, the FJ aircraft was flown so that its track was approximately perpendicular to a line between the M-33 radar station and the ionized cloud. The cloud lay between the aircraft and the radar station. The aircraft was positioned by Tacan during the standby phase of the flight and visually by the pilot from H + 1 to H + 6 minutes. During this latter phase of the flight, the aircraft was skin tracked by the M-33 radar set. Figure 2.4 shows the planned flight pattern for the FJ aircraft for Shot Priscilla.

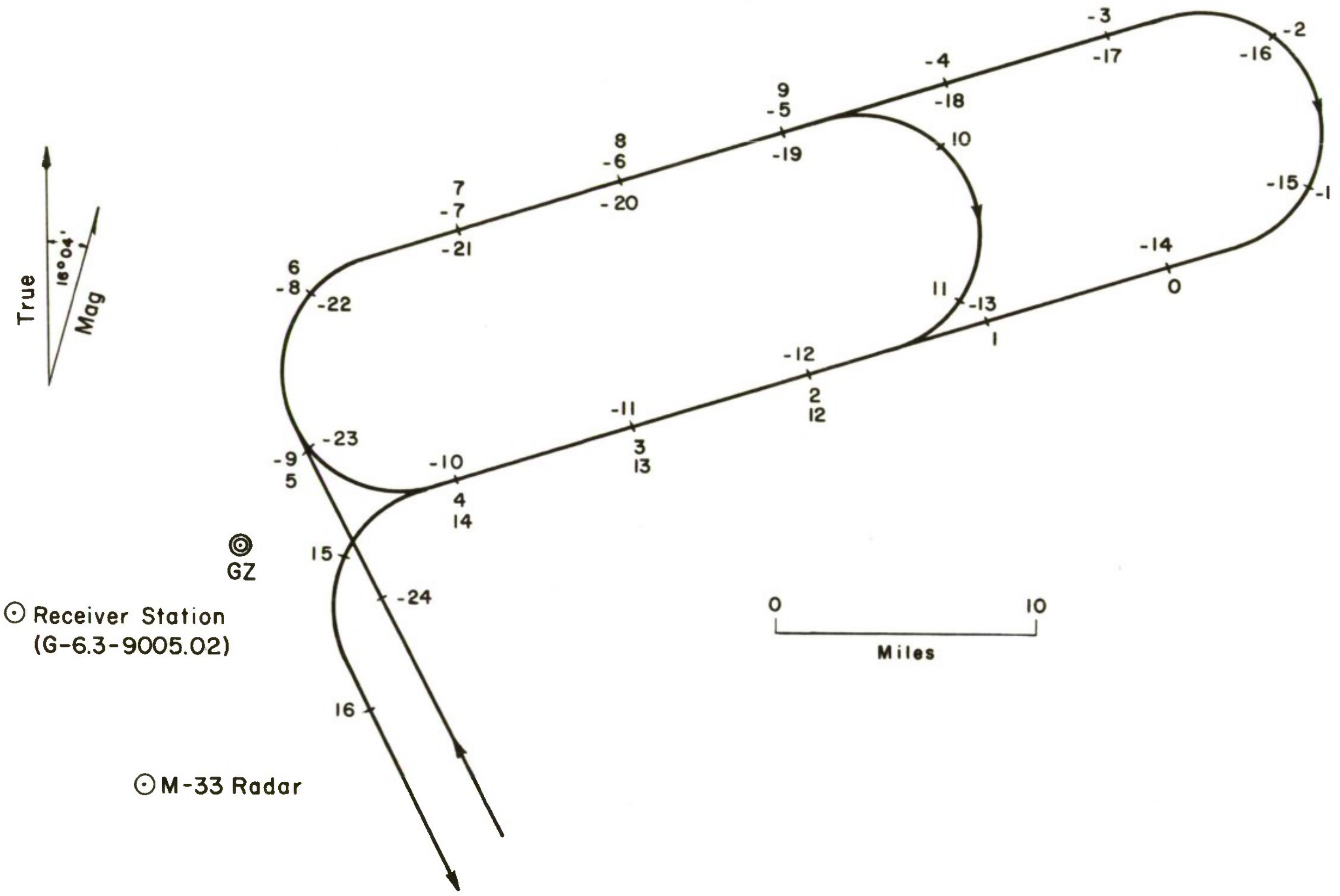

Figure 2.1 No-wind flight pattern for A4D-1 aircraft for Shot Franklin. Time in minutes before and after detonation indicated on pattern. Ground speed of aircraft 420 knots.

2.2 AIRCRAFT INSTRUMENTATION

2.2.1 Transmitters. All airborne equipment required for this project except a pilot's control box was carried in a 150-gallon fuel tank mounted under the fuselage of the A4D-1 aircraft. The same plugs and wiring as are used for the Navigational Radio Stores Assembly (NAVPAC) were utilized. Two control boxes, C760A/A and Douglas 45-44401-501, which are used with the NAVPAC were replaced by a box containing all necessary controls for operation of the airborne equipment. Table 2.1 gives some characteristics of the transmitting equipment.

TABLE 2.1 CHARACTERISTICS OF TRANSMITTING EQUIPMENT

Frequency	Type of Emission	Peak Power	Polarization	Antenna Gain
Mc				decibels
4.085	2PO	75	—	—
19.2275	2PO	75	—	—
160	3000PO	1,000	Vertical	0
960	3000PO	1,000	Vertical	0
3,100	3000PO	1,000	Vertical	12
9,245	3000PO	40,000	Vertical	12

The transmitters were enclosed in a pressurized capsule approximately $6\frac{1}{2}$ feet long and $12\frac{1}{2}$ inches in diameter. Airborne instrumentation consisted of a power meter for each transmitter, an altimeter, an artificial horizon, primary voltage monitors and a clock. A camera operating at about one frame every two seconds recorded the readings of the instruments. The equipment was designed to meet the environmental, electrical, and mechanical requirements of Specification MIL–I–5400. Figure 2.5, 2.6, 2.7, 2.8, amd 2.9 show various views of the airborne equipment.

2.2.2 Antennas. Directional horn antennas for the X-band and S-band transmissions were mounted in the nose section of the pod behind a radome, both with a 10-degree downward tilt. A blade type AS-133 IFF antenna was mounted on the centerline of the pod about three feet from the nose for the L-band frequency. A stub antenna tuned to 160 Mc was mounted on the centerline of the pod about six feet from the nose section.

TABLE 2.2 CHARACTERISTICS OF AIRBORNE ANTENNAS

Frequency	Vertical Beam Width	Horizontal Beam Width	Polarization	Gain
Mc	degrees	degrees		decibels
4.085	—	—	—	—
19.2275	—	—	—	—
180	90	180	Vertical	0
960	90	180	Vertical	0
3,100	40	30	Vertical	12
9,245	43	28	Vertical	12

Brass bars about 8 feet long were mounted horizontally a little above the centerline of the pod about four inches from the pod. These were excited at one end; the other end was an open circuit. When these brass bars were properly matched, they caused the pod and therefore the aircraft to act as a radiator. It was difficult to calculate the principal direction of polarization; however, sufficient energy was radiated to give a signal level about 30 decibels above noise at maximum range (40 miles) for the 20-Mc transmitter and about 10 to 15 decibels above noise for the 4-Mc unit. Table 2.2 gives some characteristics of the airborne antennas.

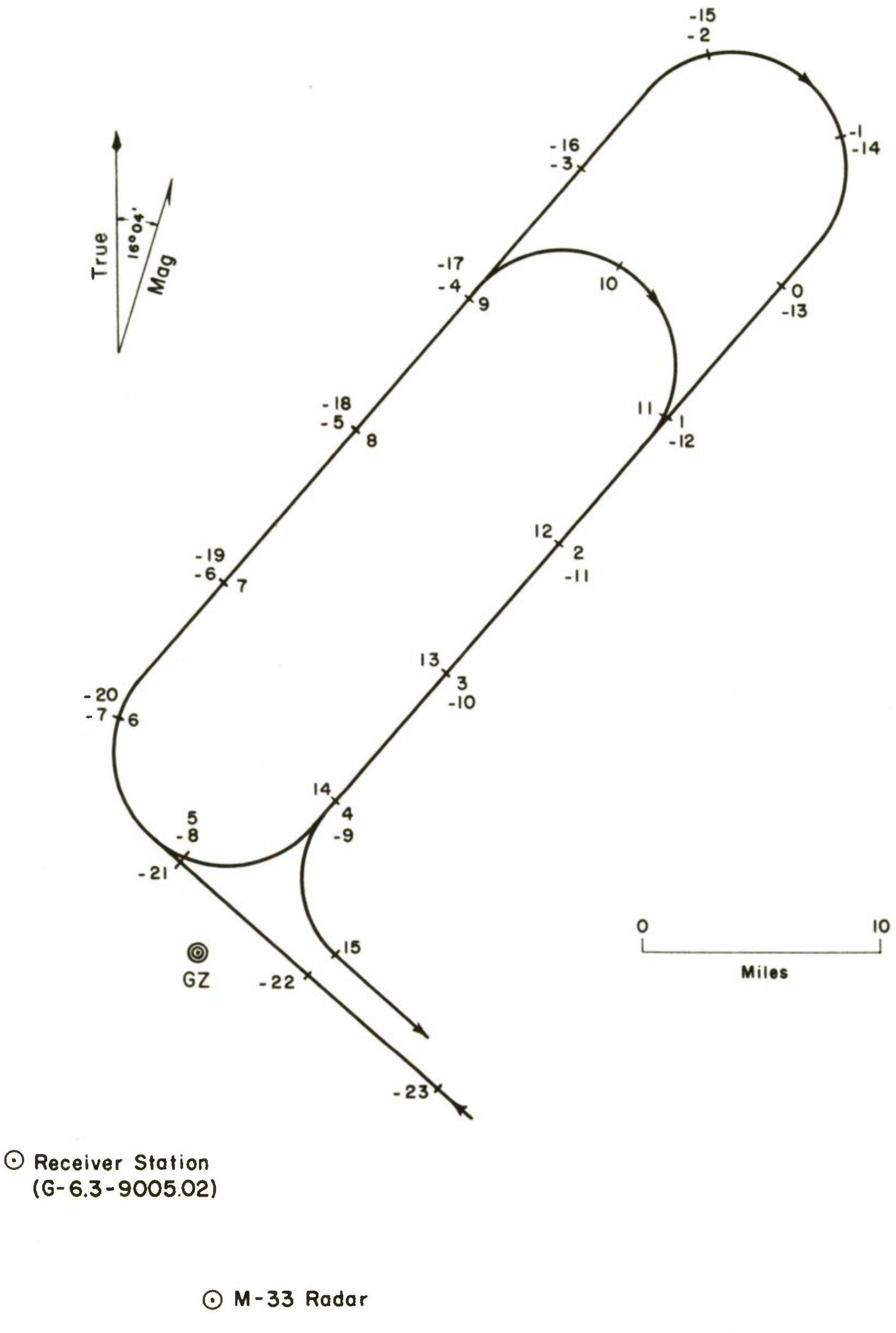

Figure 2.2 No-wind flight pattern for A4D-1 aircraft for Shot Lassen. Time in minutes before and after detonation indicated on pattern. Ground speed of aircraft 420 knots.

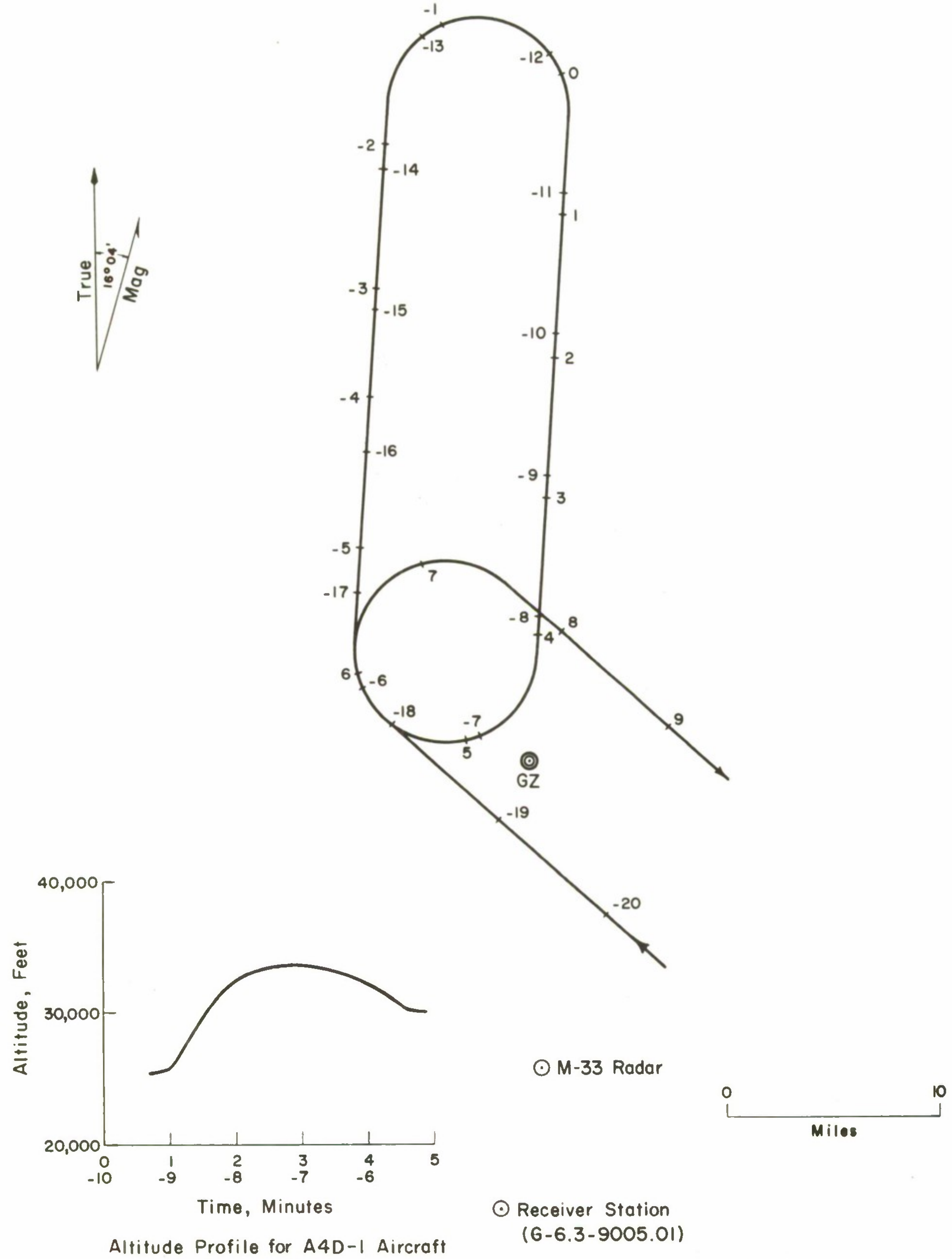

Figure 2.3 No-wind flight pattern for A4D-1 aircraft for Shot Wilson. Time in minutes before and after detonation indicated on pattern. Ground speed of aircraft 400 knots.

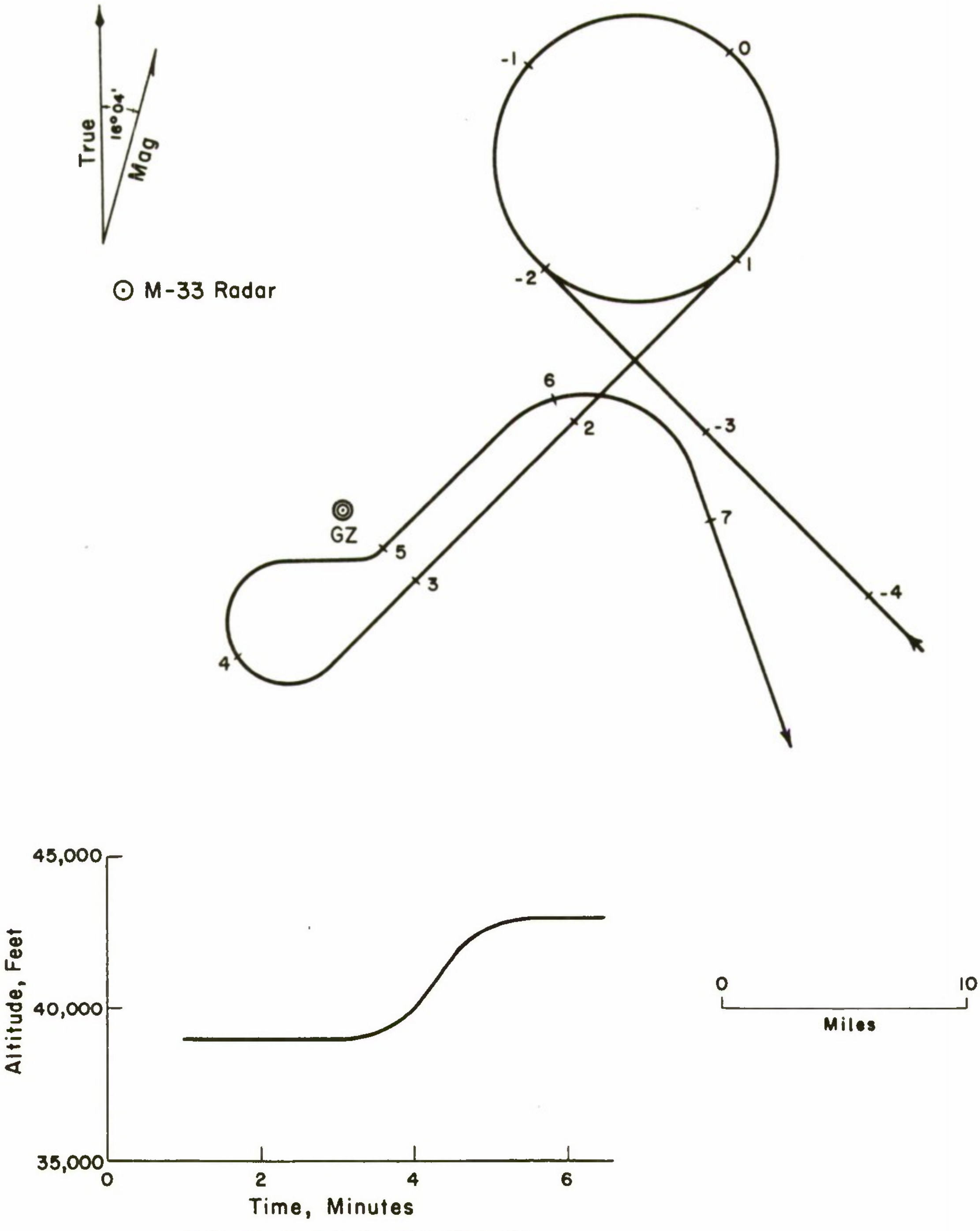

Altitude Profile for FJ Aircraft

Figure 2.4 No-wind flight pattern for FJ aircraft for Shot Priscilla. Time in minutes before and after detonation indicated on pattern. Ground speed of aircraft 425 knots.

2.3 GROUND INSTRUMENTATION

Two trailer vans located about 500 feet apart housed duplicate sets of receiving equipment. Variations in field strength caused by reflections were compensated for by combining the data from the two receiving stations. Figures 2.10 and 2.11 show interior and exterior views of the receiving vans.

2.3.1 Receivers. Receivers from the X, S, L, and A bands were procured from Airborne Instruments Laboratory. These receivers were built up of commercial subassemblies, i.e., local oscillators from General Radio, Inc., power supplies from Lamda, Inc., etc. The contractor assembled these parts into rack-mounted equipment. Collins 51J4 receivers were utilized for the two HF frequencies. Since all these receivers were built to commercial standards, care to provide reasonable environmental

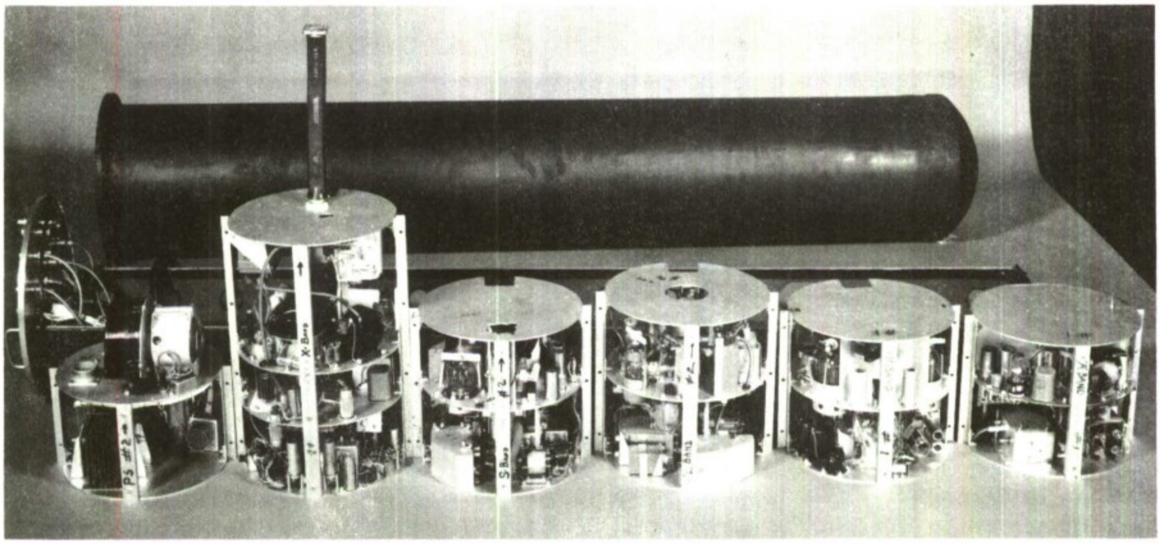

Figure 2.5 Airborne equipment showing replaceable transmitter units, cradle, and pressure tight capsule.

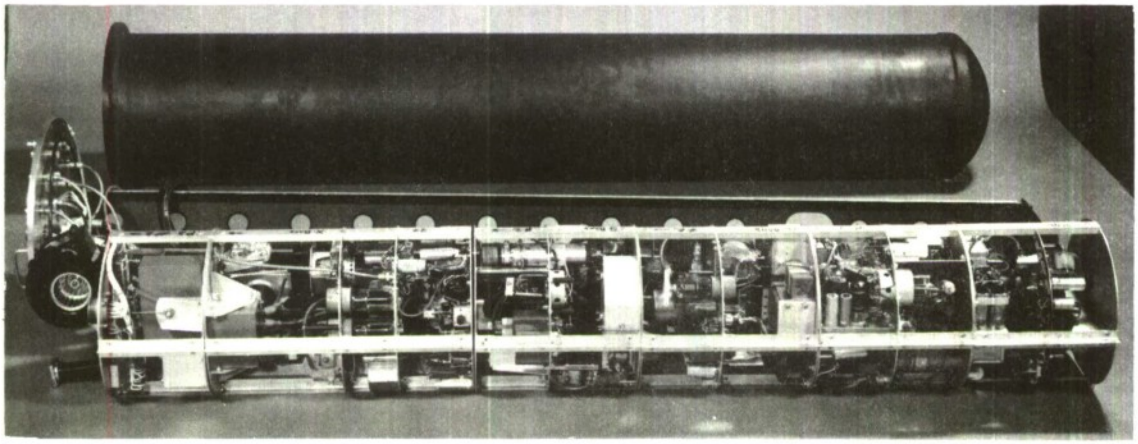

Figure 2.6 Airborne equipment showing transmitter assembled in cradle, and pressure tight capsule.

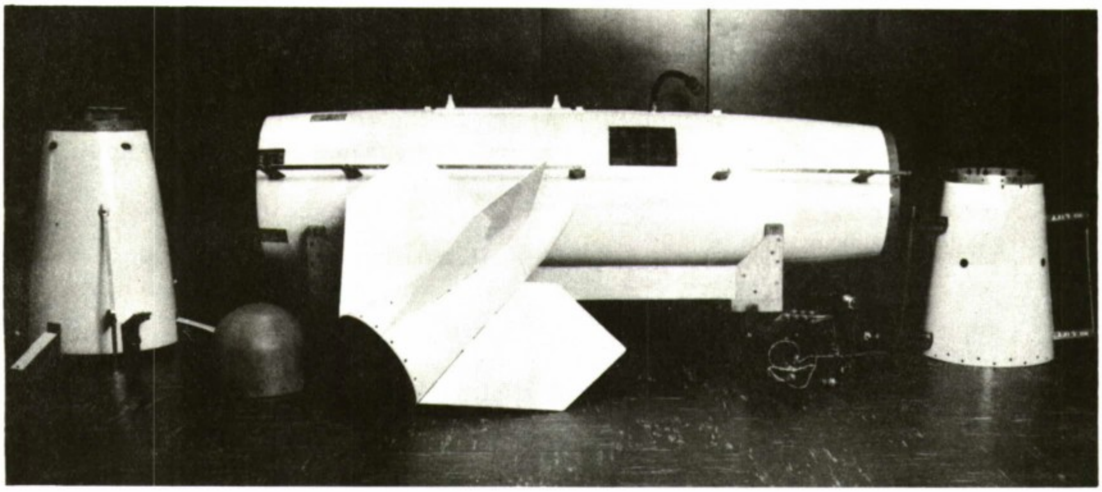

Figure 2.7 Airborne equipment showing sections of pod.

conditions was necessary to ensure satisfactory results. Table 2.3 gives pertinent data regarding these receivers.

Outputs from these receivers were integrated and recorded. The integrators were essentially vacuum tube voltmeters with a time constant of about 0.05 second.

2.3.2 Antennas. Directional antennas mounted on rotatable masts affixed to the trailer vans were used for all frequencies of interest except the 4.085-Mc frequency. Long-wire antennas from 50-foot masts to each trailer were used for the lowest frequency. Characteristics of these antennas are shown in Table 2.4.

2.4 MAINTENANCE FACILITY

A maintenance truck stationed at Indian Springs Air Force Base was utilized as a workshop for calibration and repair of the aircraft installation for Project 6.3.

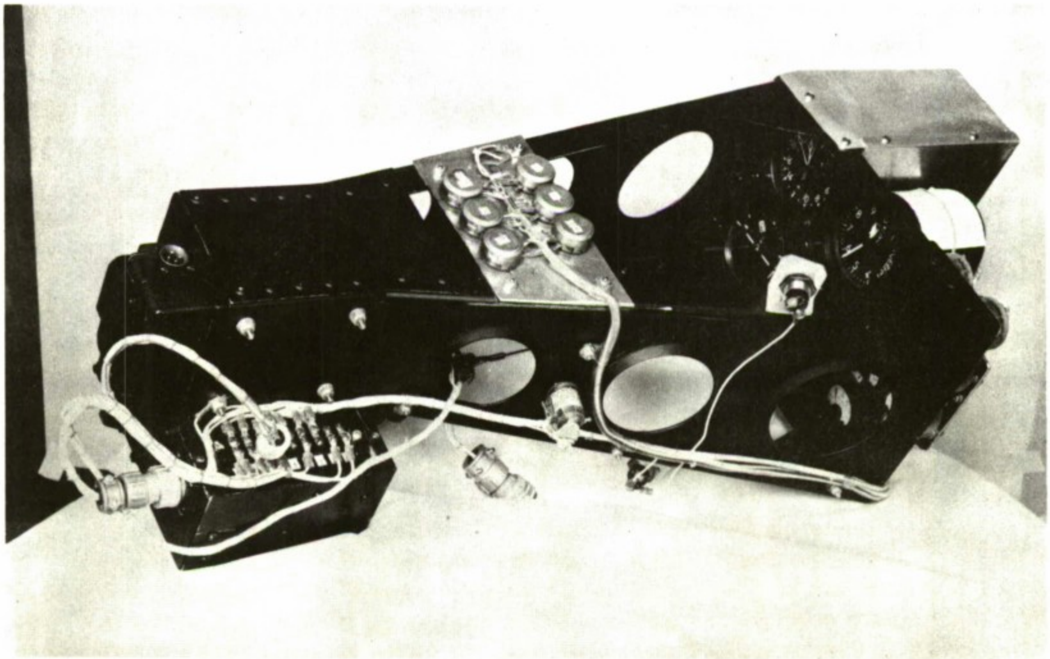

Figure 2.8 Airborne equipment showing instrument theater.

2.5 DESCRIPTION OF DATA

2.5.1 Attenuation Measurement. Outputs from the receivers were integrated and presented as voltages on Varian G-11 Strip Chart Recorders. These recorders had a response time of about 0.1 second. The receivers had the limiting dynamic ranges in the receiving-recording chains. Tests showed that the system was capable of recording to a precision of ± 1 decibel.

TABLE 2.3 CHARACTERISTICS OF RECEIVERS

Frequency	Band Width	Noise Figure	Dynamic Range
Mc	Mc	decibels	decibels
4.085	10^{-3}	10	60
19.2275	10^{-3}	10	80
180	3	10	80
960	5	10	50
3,100	5	10	50
9,245	5	10	55

Stability of the transmitting and receiving systems had to be assured for at least 35 minutes. The transmitter power outputs were continuously monitored and recorded, and it was shown by several tests that the calibration of the receivers would not change appreciably for one hour.

TABLE 2.4 CHARACTERISTICS OF GROUND-BASED ANTENNAS

Frequency	Vertical Beam Width	Horizontal Beam Width	Polarization	Gain
Mc	degrees	degrees		decibels
4.085	90	Omnidirectional	Horizontal	0
19.2275	45	150	Vertical	8
160	30	80	Vertical	13
960	80	30	Vertical	12
3,100	40	30	Vertical	12
9,245	43	28	Vertical	12

The receiving-recording chain was calibrated before and after each run. Further corrections due to power drift of the transmitters as recorded by a camera were planned, but experience showed that the power drift in the transmitters was negligible over a period of one hour.

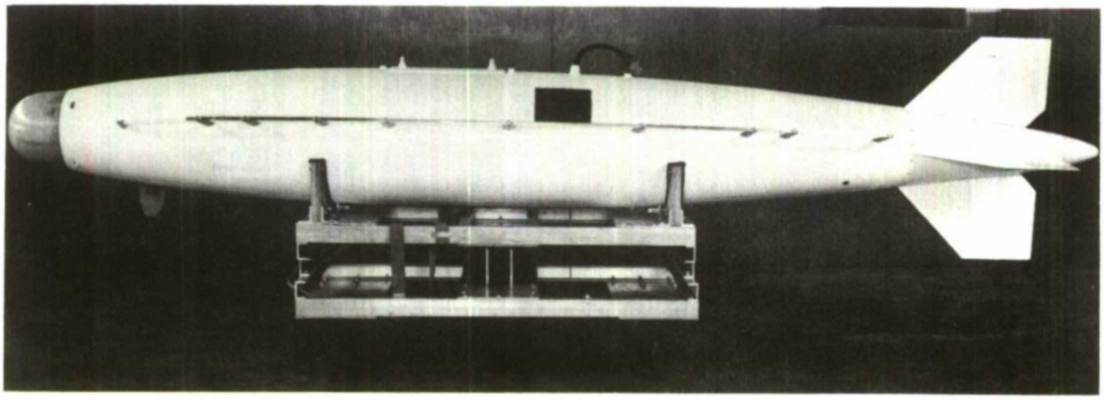

Figure 2.9 Airborne equipment showing assembled pod.

A calibration run established signal strength versus time; then a similar run with the ionized cloud interposed between the aircraft and the ground station was made.

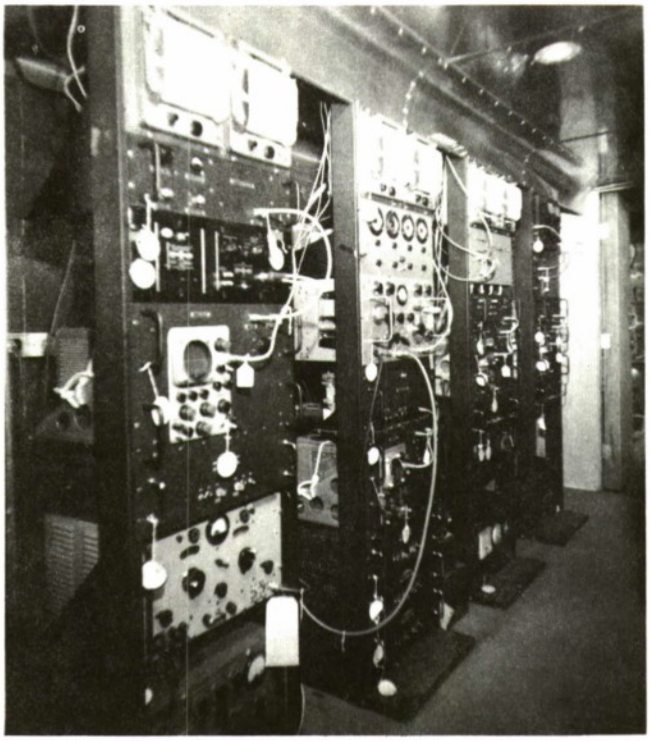

Figure 2.10 Interior view of ground receiver van showing receivers, monitors, and recorders.

Curves were plotted for both (designated A and B, respectively). Since the aircraft position was never exactly as predicted, the time axes of both curves were expanded or contracted in order that points on the calibration-run curve (A) would correspond in distance to points on the interposed-cloud curve (B). The difference between Curves A and B represented attenuation versus distance from the aircraft to the ground receivers. The distance scale was then referred to time after detonation.

2.5.2 Radar Skin Tracking. A check to determine if the ionized cloud would affect the return for an X-band radar was made on Shot Priscilla. An operator observed the radar return on an A-scope presentation. Motion pictures were taken of this display as the FJ aircraft flew so that the ionized cloud lay between the M-33 radar and the aircraft.

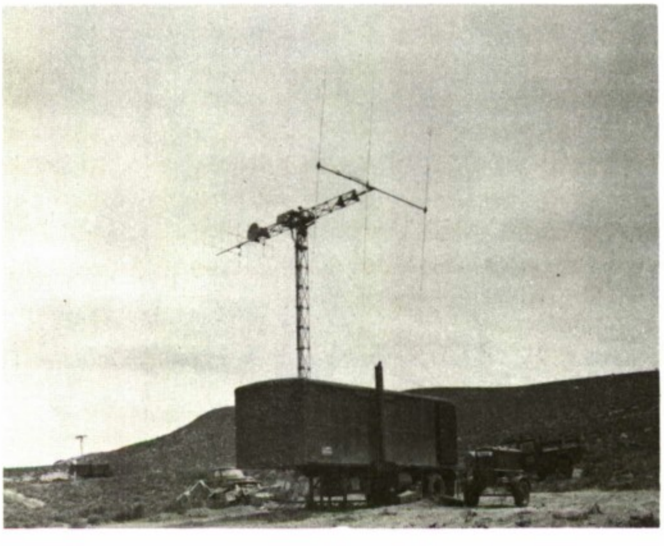

Figure 2.11 Exterior view of two ground receiver vans.

Chapter 3

RESULTS

3.1 ATTENUATION MEASUREMENTS

On all shot participations the equipment utilized for attenuation measurements functioned properly. The pilot of the aircraft was able to accomplish visual positioning, as planned, without difficulty. Except for the 4.085-Mc channel, the records obtained indicated no attenuation of the frequencies tested due to propagation of the radio signals through the ionized clouds of Franklin, Lassen, and Wilson in the period H + 1 to H + 4 minutes.

Figure 3.1 is a photograph showing a sample of the data taken during Shot Wilson of a record of the S-band signal. The bottom chart shows the time from H – 10 to H – 7 minutes—the calibration run. The top chart shows the time from H + 1 to H + 4 minutes—the interposed-cloud run. The calibration scale for the lower chart is at the right, while the calibration scale for the upper chart is at the left.

Interference on the 4.085-Mc channel on each shot prevented the recording of conclusive data for that channel. However, a characteristic 400-cycle tone from the 4.085-Mc receiver was audible both during the calibration run and the run with the ionized cloud interposed. No difference in signal level was noted.

Records of the position of the A4D-1 aircraft during the participation were obtained by the M-33 radar on Shot Wilson. Edgerton, Germeshausen and Grier, Inc. (EG&G) tracked the Wilson cloud by photography to obtain after-the-fact information on its exact position. It is planned to reduce the data so obtained to confirm the relative positions of the aircraft and cloud with respect to the ground receivers. Results will be included in the final (WT) report of this project.

3.2 RADAR SKIN TRACKING

An M-33 X-band radar skin tracked the FJ aircraft from H-hour to H + 6 minutes on Shot Priscilla. The aircraft flew so that the ionized cloud was between the M-33 radar and the aircraft at H + 3 minutes and H + 5 $^1/_2$ minutes. The radar did not lose track at any time during the period from H-hour to H + 6 minutes, and no evidence of loss of signal at H + 3 minutes or H + 5 $^1/_2$ minutes was noted by the observers. Records of the flight path of the FJ aircraft were obtained from the radar, and EG&G tracked the cloud. It is planned to verify that the aircraft was behind the cloud at the times noted by the pilot. Results of this after-the-fact data will be included in the final (WT) report of this project.

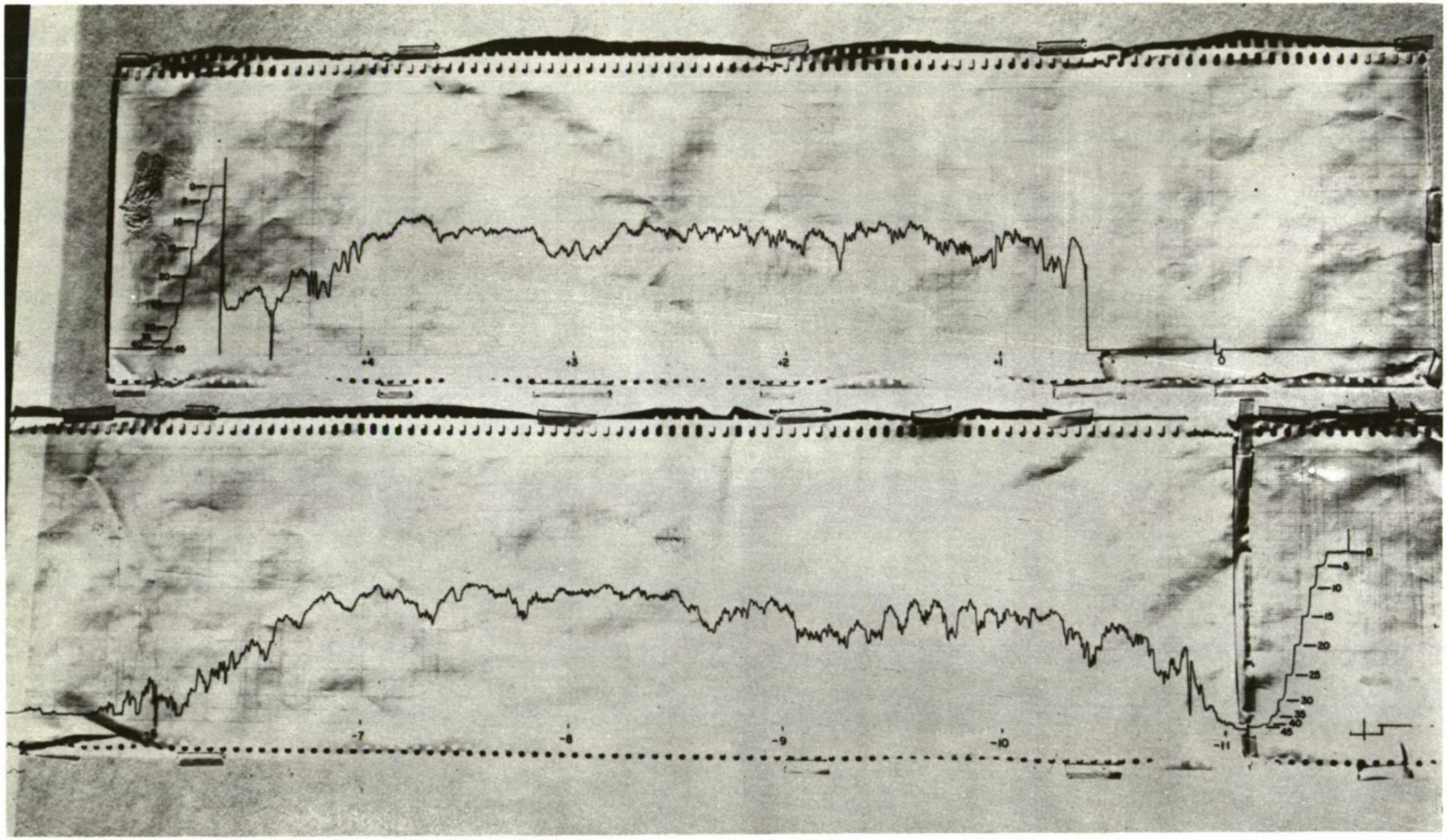

Figure 3.1 Record of S-band signal taken during Shot Wilson.

Chapter 4

DISCUSSION

4.1 THEORY

The development in Section 1.3 applies only in an infinite, homogeneous medium with both transmitting and receiving systems within the medium. This was not the case in this experiment, since both transmitters and receivers were outside the ionized medium and the radio energy must pass through the boundary layer twice. However, that theory serves as a basic approach, since the geometry, boundary conditions and ionization gradient within the cloud would be very difficult to determine.

The leading edge of a sharp pulse was used to measure signal strength. This greatly reduced the effect of reflections and any multipaths on the recorded signal strength, since only the shortest path signal was recorded.

4.2 INTERFERENCE

Difficulty with interference on the 4-Mc channel was noted only during the period from about 0100 until 0500. Checks from 0900 until 1800 showed at least 15 decibels less interference than during the pre-dawn period. This phenomenon was probably due to the fact that the ground wave was highly attenuated because of the terrain, but that the sky wave was not. Since the sky wave was strong during the time of the detonation, more interference during the pre-dawn period than during the day could be expected.

There was too little safety factor in the 4-Mc channel, due to the difficulty of designing a low-frequency antenna in the limited space available. Since the A4D-1 aircraft were also used as effects aircraft for another project, no external antenna structures could be fitted.

4.3 FREQUENCY DRIFT

Some frequency drift in the S- and X-band transmitters and in the X-band receivers was noted. Careful re-tuning immediately before recording produced satisfactory results.

4.4 CALCULATIONS

Due to the lack of attenuation noted, calculation of the rate of removal of electrons by recombination could not be made.

Chapter 5

CONCLUSIONS and RECOMMENDATIONS

5.1 CONCLUSIONS

From one to four minutes after a nuclear detonation of 10-kt yield or less, there is no attenuation of the radio signals tested by this project as a result of passing through the ionized cloud.

An X-band fire control radar will track a small jet aircraft with no noticeable loss of signal when the aircraft is screened from the radar by the ionized cloud of a 40-kt detonation.

5.2 RECOMMENDATIONS

No further electromagnetic-attenuation measurements of the type attempted by this project should be made for low-kiloton-range detonations during time periods later than H+ 1 minute.

REFERENCES

1. Harris, Arthur K., and Winkelman, Richard E.; "Ionispheric Effects of Nuclear Detonations"; Project 6.3, Operation Redwing, ITR–1337, October 1956; Signal Corps Engineering Laboratories, Evans Signal Laboratory, Belmar, New Jersey and Air Force Cambridge Research Center, Geophysics Research Directorate, Boston, Massachusetts; Secret, Restricted Data.

2. Caldwell, P. A., Hanscome, T. D., and Kunz, W. E.; "Attenuation of High Frequency and Ultra High Frequency by Ionization Resulting from Nuclear Explosions"; Project 6.6, Operation Redwing, ITR–1346, July 1956; Naval Research Laboratory, Washington 25, D. C.; Secret, Restricted Data.

3. Adler and Margenau; "Physics Review"; 79, 970 (1950); Unclassified.

4. Balwantz, W. W.; "Multifrequency Attenuation Measurements through Propellant Gases"; Naval Research Laboratory Report 4229; Unclassified.

5. Loeb, L. B.; "The Kinetic Theory of Gases"; McGraw–Hill Book Company, New York, N. Y.; Second Edition, 1934; Unclassified.

6. Diehl, W. S.; "Standard Atmospheric Table and Data"; NACA Report 218, 1942; Unclassified.

7. Glasstone, S., and Edlund, M. C.; "The Elements of Nuclear Reactor Theory"; D. Van Nostrand Co., New York, N. Y., 1952; Unclassified.

8. Malik, J. S.; "Summary of Information on Gamma Radiation from Atomic Weapons"; LASL Report 1620; Secret, Restricted Data.

9. Heotler, W.; "The Quantum Theory of Radiation"; Oxford University Press, Second Edition, 1944; Unclassified.

10. "Capabilities of Atomic Weapons"; TM 23–200, Revised Edition, 1 June 1955; Armed Forces Special Weapons Project; Secret, Restricted Data.

11. Whitman, F.; "Physics Review"; Volume 100, Page 572, 1956; Unclassified.

DISTRIBUTION

Military Distribution Categories 5-10 and 5-60

ARMY ACTIVITIES

1 Asst. Dep. Chief of Staff for Military Operations, D/A, Washington 25, D.C. ATTN: Asst. Executive (R&SW)
2 Chief of Research and Development, D/A, Washington 25, D.C. ATTN: Atomic Division
3 Chief of Ordnance, D/A, Washington 25, D.C. ATTN: ORDTX-AR
4 Chief Signal Officer, D/A, P&O Division, Washington 25, D.C. ATTN: SIGRD-8
5 The Surgeon General, D/A, Washington 25, D.C. ATTN: Chief, R&D Division
6- 7 Chief Chemical Officer, D/A, Washington 25, D.C.
8 The Quartermaster General, D/A, Washington 25, D.C. ATTN: Research and Development
9- 12 Chief of Engineers, D/A, Washington 25, D.C. ATTN: ENGNB
13 Chief of Transportation, Military Planning and Intelligence Div., Washington 25, D.C.
14- 16 Commanding General, Headquarters, U. S. Continental Army Command, Ft. Monroe, Va.
17 President, Board #1, Headquarters, Continental Army Command, Ft. Sill, Okla.
18 President, Board #2, Headquarters, Continental Army Command, Ft. Knox, Ky.
19 President, Board #3, Headquarters, Continental Army Command, Ft. Benning, Ga.
20 President, Board #4, Headquarters, Continental Army Command, Ft. Bliss, Tex.
21 Commanding General, Headquarters, First U. S. Army, Governor's Island, New York 4, N.Y.
22 Commanding General, Headquarters, Second U. S. Army, Ft. George G. Meade, Md.
23 Commanding General, Headquarters, Third U. S. Army, Ft. McPherson, Ga. ATTN: ACofS, G-3
24 Commanding General, Headquarters, Fourth U. S. Army, Ft. Sam Houston, Tex. ATTN: G-3 Section
25 Commanding General, Headquarters, Fifth U. S. Army, 1660 E. Hyde Park Blvd., Chicago 15, Ill.
26 Commanding General, Headquarters, Sixth U. S. Army, Presidio of San Francisco, San Francisco, Calif. ATTN: AMGCT-4
27 Commanding General, U.S. Army Caribbean, Ft. Amador, C.Z. ATTN: Cml. Off.
28 Commanding General, USARFANT & MDPR, Ft. Brooke, Puerto Rico
29 Commanding General, Southern European Task Force, APO 168, New York, N.Y. ATTN: ACofS, G-3
30 Commander-in-Chief, European Command, APO 128, New York, N.Y.
31 Commanding General, U.S. Army Forces Far East (Main), APO 343, San Francisco, Calif. ATTN: ACofS, G-3
32 Commanding General, U.S. Army Alaska, APO 942, Seattle, Wash.
33- 34 Commanding General, U.S. Army Europe, APO 403, New York, N.Y. ATTN: OPOT Div., Combat Dev. Br.
35- 36 Commanding General, U.S. Army Pacific, APO 958, San Francisco, Calif. ATTN: Cml. Off.
37- 38 Commandant, Command and General Staff College, Ft. Leavenworth, Kan. ATTN: ALLLS(AS)
39- 41 Commandant, Army War College, Carlisle Barracks, Pa. ATTN: Library
42 Commandant, The Infantry School, Ft. Benning, Ga. ATTN: C.D.S.
43 Commandant, The Artillery and Guided Missile School, Ft. Sill, Okla.
44 Secretary, The Antiaircraft Artillery and Guided Missile School, Ft. Bliss, Texas. ATTN: Maj. Gregg D. Breitegan, Dept. of Tactics and Combined Arms
45 Commandant, The Armored School, Ft. Knox, Ky.
46 Commanding General, Army Medical Service School, Brooke Army Medical Center, Ft. Sam Houston, Tex.
47 Director, Special Weapons Development Office, Headquarters, CONARC, Ft. Bliss, Tex. ATTN: Capt. T. E. Skinner
48 Commandant, Walter Reed Army Institute of Research, Walter Reed Army Medical Center, Washington 25, D. C.
49 Superintendent, U.S. Military Academy, West Point, N. Y. ATTN: Prof. of Ordnance
50 Commandant, Chemical Corps School, Chemical Corps Training Command, Ft. McClellan, Ala.
51- 52 Commanding General, Research and Engineering Command, Army Chemical Center, Md. ATTN: Deputy for RW and Non-Toxic Material
53- 54 Commanding General, Aberdeen Proving Grounds, Md. ATTN: Director, Ballistics Research Laboratory
55 Commanding General, The Engineer Center, Ft. Belvoir, Va. ATTN: Asst. Commandant, Engineer School
56 Commanding Officer, Engineer Research and Development Laboratory, Ft. Belvoir, Va. ATTN: Chief, Technical Intelligence Branch
57 Commanding Officer, Picatinny Arsenal, Dover, N.J. ATTN: ORDBB-TK
58 Commanding Officer, Frankford Arsenal, Philadelphia 37, Pa. ATTN: Col. Tewes Kundel
59 Commanding Officer, Army Medical Research Laboratory, Ft. Knox, Ky.
60- 61 Commanding Officer, Chemical Corps Chemical and Radiological Laboratory, Army Chemical Center, Md. ATTN: Tech. Library
62 Commanding Officer, Transportation R&D Station, Ft. Eustis, Va.
63 Commandant, The Transportation School, Ft. Eustis, Va. ATTN: Security and Information Officer
64 Director, Technical Documents Center, Evans Signal Laboratory, Belmar, N.J.
65 Director, Waterways Experiment Station, PO Box 631, Vicksburg, Miss. ATTN: Library
66 Director, Operations Research Office, Johns Hopkins University, 7100 Connecticut Ave., Chevy Chase, Md. Washington 15, D.C.
67- 68 Commanding General, Quartermaster Research and Development, Command, Quartermaster Research and Development Center, Natick, Mass. ATTN: CBR Liaison Officer
69- 74 Technical Information Service Extension, Oak Ridge, Tenn.

NAVY ACTIVITIES

75 Director, USMC Educational Center, Marine Corps Schools, Quantico, Va.
76- 77 Chief of Naval Operations, D/N, Washington 25, D. C. ATTN: OP-36
78 Chief of Naval Operations, D/N, Washington 25, D.C. ATTN: OP-37
79 Chief of Naval Operations, D/N, Washington 25, D.C. ATTN: OP-03EG
80 Director of Naval Intelligence, D/N, Washington 25, D.C. ATTN: OP-922V
81 Chief, Bureau of Medicine and Surgery, D/N, Washington 25, D.C. ATTN: Special Weapons Defense Div.
82 Chief, Bureau of Ordnance, D/N, Washington 25, D.C.
83 Chief of Naval Personnel, D/N, Washington 25, D.C.
84 Chief, Bureau of Ships, D/N, Washington 25, D.C. ATTN: Code 348
85 Chief, Bureau of Yards and Docks, D/N, Washington 25, D.C. ATTN: D-440
86 Chief, Bureau of Supplies and Accounts, D/N, Washington 25, D.C.
87- 88 Chief, Bureau of Aeronautics, D/N, Washington 25, D.C.

89 Chief of Naval Research, Department of the Navy Washington 25, D.C. ATTN: Code 811
90- 91 Commander-in-Chief, U.S. Pacific Fleet, Fleet Post Office, San Francisco, Calif.
92- 93 Commander-in-Chief, U.S. Atlantic Fleet, U.S. Naval Base, Norfolk 11, Va.
94- 97 Commandant, U.S. Marine Corps, Washington 25, D.C. ATTN: Code A03H
98 President, U.S. Naval War College, Newport, R.I.
99 Superintendent, U.S. Naval Postgraduate School, Monterey, Calif.
100 Commanding Officer, U.S. Naval Schools Command, U.S. Naval Station, Treasure Island, San Francisco, Calif.
101 Director, USMC Development Center, USMC Schools, Quantico, Va.
102 Commanding Officer, U.S. Fleet Training Center, Naval Base, Norfolk 11, Va. ATTN: Special Weapons School
103-104 Commanding Officer, U.S. Fleet Training Center, Naval Station, San Diego 36, Calif. ATTN: (SPWP School)
105 Commanding Officer, Air Development Squadron 5, VX-5, U.S. Naval Air Station, Moffett Field, Calif.
106 Commanding Officer, U.S. Naval Damage Control Training Center, Naval Base, Philadelphia, Pa. ATTN: ABC Defense Course
107 Commander, U.S. Naval Ordnance Laboratory, Silver Spring 19, Md. ATTN: EE
108 Commander, U.S. Naval Ordnance Laboratory, Silver Spring 19, Md. ATTN: EH
109 Commander, U.S. Naval Ordnance Laboratory, Silver Spring 19, Md. ATTN: R
110 Commander, U.S. Naval Ordnance Test Station, Inyokern, China Lake, Calif.
111 Officer-in-Charge, U.S. Naval Civil Engineering Res. and Evaluation Lab., U.S. Naval Construction Battalion Center, Port Hueneme, Calif. ATTN: Code 753
112 Commanding Officer, U.S. Naval Medical Research Inst., National Naval Medical Center, Bethesda 14, Md.
113 Director, Naval Air Experimental Station, Air Material Center, U.S. Naval Base, Philadelphia, Penn.
114 Director, U.S. Naval Research Laboratory, Washington 25, D.C. ATTN: Mrs. Katherine H. Cass
115 Director, The Material Laboratory, New York Naval Shipyard, Brooklyn, N. Y.
116 Commanding General, Fleet Marine Force, Atlantic, Norfolk, Va.
117 Commanding Officer and Director, U.S. Navy Electronics Laboratory, San Diego 52, Calif.
118-121 Commanding Officer, U.S. Naval Radiological Defense Laboratory, San Francisco, Calif. ATTN: Technical Information Division
122 Officer-in-Charge, Special Weapons Supply Depot, U.S. Naval Supply Center, Norfolk 11, Va.
123 Commanding Officer and Director, David W. Taylor Model Basin, Washington 7, D.C. ATTN: Library
124 Commander, U.S. Naval Air Development Center, Johnsville, Pa.
125 Commanding Officer, Clothing Supply Office, Code 1D-0, 3rd Avenue and 29th St., Brooklyn, N.Y.
126 Commandant, U.S. Coast Guard, 1300 E. St. N.W., Washington 25, D.C. ATTN: (OIN)
127 Commanding General, Fleet Marine Force, Pacific, Fleet Post Office, San Francisco, Calif.
128 CINCPAC, Pearl Harbor, TH
129 Commander, Norfolk Naval Shipyard, Portsmouth 8, Va. ATTN: Code 270
130-134 Technical Information Service Extension, Oak Ridge, Tenn. (Surplus)

AIR FORCE ACTIVITIES

135 Asst. for Atomic Energy Headquarters, USAF, Washington 25, D.C. ATTN: DCS/O
136 Asst. for Development Planning, Headquarters, USAF, Washington 25, D.C.
137 Deputy for Materiel Atomic Energy Control, Asst. for Materiel Program Control, DCS/M, Headquarters, USAF, Washington 25, D. C. ATTN: AFMPC-AE
138 Director of Operations, Headquarters, USAF, Washington 25, D.C. ATTN: Operations Analysis
139 Director of Operations, Headquarters, USAF, Washington 25, D.C.
140 Director of Plans, Headquarters, USAF, Washington 25, D.C. ATTN: War Plans Div.
141 Director of Requirements, Headquarters, USAF, Washington 25, D.C. ATTN: AFDRQ-SA/M
142 Director of Research and Development, DCS/D, Headquarters, USAF, Washington 25, D.C. ATTN: Combat Components Div.
143-144 Director of Intelligence, Headquarters, USAF, Washington 25, D.C. ATTN: AFOIN-IB2
145 The Surgeon General, Headquarters, USAF, Washington 25, D.C. ATTN: Bio. Def. Br., Pre. Med. Div.
146 Asst. Chief of Staff, Intelligence, Headquarters, U.S. Air Forces-Europe, APO 633, New York, N.Y. ATTN: Directorate of Air Targets
147 Commander, 497th Reconnaissance Technical Squadron (Augmented), APO 633, New York, N.Y.
148 Commander, Far East Air Forces, APO 925, San Francisco, Calif. ATTN: Special Asst. for Damage Control
149-150 Commander, Alaskan Air Command, APO 942, Seattle, Wash. ATTN: AAOTN
151 Commander, Northeast Air Command, APO 862, New York, N.Y.
152 Commander-in-Chief, Strategic Air Command, Offutt Air Force Base, Omaha, Nebraska. ATTN: Special Weapons Branch, Inspector Div., Inspector General
153 Commander, Tactical Air Command, Langley AFB, Va. ATTN: Documents Security Branch
154 Commander, Air Defense Command, Ent AFB, Colo.
155-156 Research Directorate, Headquarters, Air Force Special Weapons Center, Kirtland Air Force Base, New Mexico, ATTN: Blast Effects Res.
157 Commander, Air Materiel Command, Wright-Patterson AFB, Dayton, O. ATTN: MCSW
158 Assistant Chief of Staff, Installations, Headquarters, USAF, Washington 25, D.C. ATTN: AFCIE-E
159 Commander, Air Research and Development Command, PO Box 1395, Baltimore, Md. ATTN: RDDN
160 Commander, Air Proving Ground Command, Eglin AFB, Fla. ATTN: Adj./Tech. Report Branch
161-162 Director, Air University Library, Maxwell AFB, Ala.
163-170 Commander, Flying Training Air Force, Waco, Tex. ATTN: Director of Observer Training
171 Commander, Crew Training Air Force, Randolph Field, Tex. ATTN: 2GTS, DCS/O
172-173 Commandant, Air Force School of Aviation Medicine, Randolph AFB, Tex.
174-179 Commander, Wright Air Development Center, Wright-Patterson AFB, Dayton, O. ATTN: WCOSI
180-181 Commander, Air Force Cambridge Research Center, LG Hanscom Field, Bedford, Mass. ATTN: CRQST-2
182-184 Commander, Air Force Special Weapons Center, Kirtland AFB, N. Mex. ATTN: Library
185 Commander, Lowry AFB, Denver, Colo. ATTN: Department of Special Weapons Training
186 Commander, 1009th Special Weapons Squadron, Headquarters, USAF, Washington 25, D.C.
187-188 The RAND Corporation, 1700 Main Street, Santa Monica, Calif. ATTN: Nuclear Energy Division
189 Commander, Second Air Force, Barksdale AFB, Louisiana. ATTN: Operations Analysis Office
190 Commander, Eighth Air Force, Westover AFB, Mass. ATTN: Operations Analysis Office
191 Commander, Fifteenth Air Force, March AFB, Calif. ATTN: Operations Analysis Office
192 Commander, Western Development Div. (ARDC), PO Box 262, Inglewood, Calif. ATTN: WDSIT, Mr. R. G. Weitz
193-197 Technical Information Service Extension, Oak Ridge, Tenn. (Surplus)

OTHER DEPARTMENT OF DEFENSE ACTIVITIES

198 Executive Secretary, Joint Chiefs of Staff, Washington 25, D.C.
199-200 Asst. Secretary of Defense, Research and Development, D/D, Washington 25, D.C. ATTN: Tech. Library
201 U.S. Documents Officer, Office of the U.S. National Military Representative, SHAPE, APO 55, New York, N.Y.
202 Director, Weapons Systems Evaluation Group, OSD, Rm 2E1006, Pentagon, Washington 25, D.C.
203 Asst. for Civil Defense, OSD, Washington 25, D.C.
204 Armed Services Explosives Safety Board, D/D, Building T-7, Gravelly Point, Washington 25, D.C.
205 Executive Secretary, Military Liaison Committee, PO Box 1814, Washington 25, D.C.

206 Commandant, National War College, Washington 25, D.C. ATTN: Classified Records Library

207 Commandant, Armed Forces Staff College, Norfolk 11, Va. ATTN: Secretary

208 Commandant, Industrial College of the Armed Forces, Ft. Lesley J. McNair, Washington 25, D.C.

209 Commander, Field Command, Armed Forces Special Weapons Project, PO Box 5100, Albuquerque, N. Mex.

210 Commander, Field Command, Armed Forces Special Weapons Project, PO Box 5100, Albuquerque, N. Mex. ATTN: Technical Training Group

211-215 Commander, Field Command, Armed Forces Special Weapons Project, P.O. Box 5100, Albuquerque, N. Mex. ATTN: Deputy Chief of Staff, Weapons Effects Test

216-226 Chief, Armed Forces Special Weapons Project, Washington 25, D.C. ATTN: Documents Library Branch

227 Commanding General, Military District of Washington, Room 1543, Building T-7, Gravelly Point, Va.

228-232 Technical Information Service Extension, Oak Ridge, Tenn. (Surplus)

ATOMIC ENERGY COMMISSION ACTIVITIES

233-235 U.S. Atomic Energy Commission, Classified Technical Library, 1901 Constitution Ave., Washington 25, D.C. ATTN: Mrs. J. M. O'Leary (For DMA)

236-237 Los Alamos Scientific Laboratory, Report Library, PO Box 1663, Los Alamos, N. Mex. ATTN: Helen Redman

238-242 Sandia Corporation, Classified Document Division, Sandia Base, Albuquerque, N. Mex. ATTN: H. J. Smyth, Jr.

243-245 University of California Radiation Laboratory, PO Box 808, Livermore, Calif. ATTN: Clovis G. Craig

246 Weapon Data Section, Technical Information Service Extension, Oak Ridge, Tenn.

247-265 Technical Information Service Extension, Oak Ridge, Tenn. (Surplus)

CONFIDENTIAL

This document consists of 1 page

No. 187 of 265 copies, Series A

December 16, 1957

ERRATA SHEET FOR ITR-1437

86124
RT
Physics
c. 1

ATTENUATION OF ELECTROMAGNETIC RADIATION THROUGH AN IONIZED MEDIUM (OPERATION PLUMBBOB PRELIMINARY REPORT, PROJECT 6.3)

Page 9, Section 1.3, second paragraph.

FOR: $e\,\bar{E}_o^{-i\omega t}$

READ: $e\,\bar{E}_o \exp(-i\omega t)$

Page 9, Equation (1.1).

FOR: $\frac{md\bar{V}}{dt} + \frac{m\bar{V}}{\tau} = e\,\bar{E}_o^{-i\omega t}$

READ: $m\,\frac{d\bar{V}}{dt} + \frac{m\bar{V}}{\tau} = e\,\bar{E}_o \exp(-i\omega t)$

Page 10, Equation (1.2).

FOR: $\bar{V} = \frac{e\,\bar{E}_o^{-i\omega t}}{m\left(\frac{1}{\tau} - i\omega\right)}$

READ: $\bar{V} = \frac{e\,\bar{E}_o \exp(-i\omega t)}{m\left(\frac{1}{\tau} - i\omega\right)}$

This material contains information affecting the national defense of the United States within the meaning of the espionage laws Title 18, U. S. C., Secs. 793 and 794, the transmission or revelation of which in any manner to an unauthorized person is prohibited by law.

DISTRIBUTION

Military Categories 5-10 and 5-60

USAEC TECHNICAL INFORMATION SERVICE EXTENSION, P. O. BOX 401,
OAK RIDGE, TENNESSEE

CONFIDENTIAL

FORMERLY RESTRICTED DATA

Postal Registry No. 14153

CONFIDENTIAL

FORMERLY RESTRICTED DATA

CONFIDENTIAL